CHEMICAL ENGINEERING TRANSACTIONS
VOL. 86, 2021
A publication of AIDIC
The Italian Association of Chemical Engineering
Online at www.cetjournal.it
Guest Editors: Sauro Pierucci, Jiří Jaromír Klemeš

ISBN 978-88-95608-84-6; **ISSN** 2283-9216
DOI: 10.3303/CET2186218

Facile Synthesis of Nickel-carbon Nanotube Composite from Petrochemical Waste Oil

Chosel P. Lawagon[a,*], Tawatchai Charinpanitkul[b]

[a]Chemical Engineering, College of Engineering, University of Mindanao, Matina, Davao City 8000, Philippines
[b]Center of Excellence in Particle Technology, Department of Chemical Engineering, Faculty of Engineering, Chulalongkorn University, Bangkok 10330, Thailand
clawagon@umindanao.edu.ph

Upcycling route for handling petrochemical waste oil (PWO) is a sustainable alternative to its costly and complex treatment. However, the mishandling of PWO can lead to environmental and health hazards. Finding other valuable usages for PWO is a viable long-term solution. Hence, a new approach for synthesizing carbon nanotube-metal composite from PWO is significantly beneficial because of its environmental and economic benefits. Herein, simple catalytic vapor deposition (CVD) was used to synthesize carbon nanotubes (CNTs) from PWO. Optimal conditions for the CNT synthesis were determined by varying the temperature (900 – 950 ^{o}C) and catalyst to carbon precursor ratio at a preset residence time (0.5 h). It was observed that CNTs diameter increased with increasing temperature, but carbon yield decreased. On the other hand, nickel (Ni) nano-layer was deposited on the CNT surface by electroless plating (ELP). The effect of temperature (30 – 70 ^{o}C) during ELP on the thickness of the coating and morphological structure was also investigated. Prior to ELP, CNT's surface was treated with H_2O_2 (1:50 wt. ratio) at 60^{o}C for 2h to improve its dispersibility in an aqueous solution. It was then further sensitized and activated to make it an autocatalytic substrate. As the temperature increased, the amount of Ni deposited into the CNT's surface also increased. At temperature > 60 ^{o}C the morphology of the CNT significantly changed. Still, Ni-CNT's structural stability and integrity were maintained even after Ni deposition proving that ELP is a facile approach for the synthesis of a metal-carbon framework.

1. Introduction

The petrochemical industry has become an integral part of civilization and progress. However, it also caused the generation of ~one million tons of waste oil in South Korea alone (Ko et al., 2016) and a significantly large amount worldwide each year (Lam et al., 2016), which are classified as hazardous wastes posing health and environmental risks (Singh et al., 2017). Processing this petrochemical waste oil (PWO) is complex and costly. Some of the employed processes caused secondary pollution due to a large amount of greenhouse gases released into the atmosphere (Liu et al., 2019).

A sustainable approach to handling PWO is finding a valuable alternative usage, such as in carbon nanotube (CNT) synthesis. CNT has been utilized in several promising applications due to its excellent chemical, electrical, mechanical, thermal, and optical properties (Hernández-Vargas et al., 2015). Hence, it has since become a significant driver and element in material processing for advanced technological innovations (Zhang, 2018). CNTs also have a projected market value of USD 9.85 billion by 2023 (Dang et al., 2019). Thereby, PWO to CNTs is a very attractive upcycling route

Herein, PWO was repurposed to produce CNT in a facile one-step process of catalytic vapor deposition (CVD). Heavy fuel oil (HFO) was used as an ideal representation of PWO for this purpose. Eventually, the as-prepared CNTs were used as support for Nickel (Ni) electroless plating, which can then be possibly used in several catalytic applications.

Paper Received: 5 September 2020; Revised: 26 February 2021; Accepted: 16 April 2021
Please cite this article as: Lawagon C.P., Charinpanitkul T., 2021, Facile Synthesis of Nickel-carbon Nanotube Composite from Petrochemical Waste Oil, Chemical Engineering Transactions, 86, 1303-1308 DOI:10.3303/CET2186218

2. Experimental

2.1 Materials

Heavy fuel oil (HFO) used as carbon precursor was from PTT Oil and Retail Business Public Company Ltd (Batch No. TA 01/19/0004). Ferrocene (98% $Fe(C_5H_5)_2$, Sigma Aldrich USA) was used as a catalyst. Hydrogen peroxide (30% H_2O_2, QReC, New Zealand) and hydrochloric acid (37% HCl, QReC, New Zealand) were used to purify the as-synthesized CNTs. Tin(II) chloride (> 95% $SnCl_2$, Ajax Finechem Pty Ltd, Australia) and silver nitrate (99.9% $AgNO_3$, GEMChem Chemical & Laboratory reagents, India) were used for sensitization and activation of CNTs. Nickel(II) chloride hexahydrate (99% $NiCl_2.6H_2O$, CARLO ERBA reagent SAS, France), sodium hypophosphite monohydrate (99% $NaH_2PO_2.H_2O$ CARLO ERBA reagent SAS, France), sodium acetate (99% CH_3COONa, LOBA CHEMIE PVT.LTD, India), sodium citrate dihydrate (99.0% $Na_3C_6H_5O_7.2H_2O$, Cameleon reagent, Japan) were used for preparing the electroless solution. Ammonia (30% NH_3, AppliChem Panreac, Germany) was used to adjust the temperature of the electroless solution. All chemicals were used as received.

2.2 Synthesis of carbon nanotubes

CNTs were prepared by catalytic vapor deposition (CVD) using HFO and ferrocene as carbon precursor and catalysts at 1:10 molar ratio with N_2 carrier gas (100 mL h^{-1}). The temperature was varied (900 – 950 ^oC). HFO and ferrocene were loaded in a ceramic boat, put at the quartz tube entrance, moved inside the reactor when the set temperature was reached, and left there for 0.5 h. Self-assembly and catalytic growth reactions of CNTs took place in the middle zone of the quartz tube reactor (40 mm outer diameter, 65 cm length).

2.3 Nickel electroless plating

Synthesized CNTs were purified by sonicating in 2:1 (v/v) H_2O_2 and HCl mixture for 5 h at 60 ^oC. Sensitization was done by immersing in a 60 mL of 0.1M HCl-0.1 M $SnCl_2$ solution at 15 ^oC for 30 minutes, followed by rinsing with DI water. It was then activated with 60 mL of 0.25M HCl-0.0028M $AgNO_3$ solution at 15 ^oC for 30 mins. Samples were rinsed with DI and were added in 30 mL electroless solution (pH at 8.5) containing $NiCl_2.6H_2O$ (18 g L^{-1}), $NaH_2PO_2.H_2O$ (16 g L^{-1}), CH_3COONa (6 g L^{-1}), and $Na_3C_6H_5O_7.2H_2O$ (11 g L^{-1}) for 1 h at varied temperature (30, 40, 50, 60 ^oC).

2.4 Characterization

The structural property of the prepared catalyst and the surface functionalities were determined via X-ray diffraction analysis (40 kV, 40 mA, 0.03 step $count^{-1}$, Cu Kα source, Rigaku Smartlab), and Raman analysis (laser frequency of 532 nm, 2.33 eV, DXR Raman system, Thermo Fisher Scientific, America). Morphological properties were observed under Scanning Electron Microscope equipped with Energy Dispersive X-ray Spectrometer (SEM-EDX, Hitachi S-3500 N, Japan).

3. Results and discussions

3.1 Synthesis of CNTs from PWO

The CNTs were prepared via CVD at a temperature range of 900 – 950 ^oC where HFO and ferrocene decomposed to elemental C and Fe aided in nanotube growth. The controlled flow rate of N_2 gas carried the ferrocene and HFO vapor to synthesized CNTs within the reaction zone. FE-SEM images (Figure 1) showed that CNTs were successfully grown; however, at 900 ^oC several carbon nanoparticles around nanotubes can be observed. At 930 ^oC, a smooth and more uniform diameter distribution can be observed, while further increasing reaction temperature leads to the formation of several knots or aggregated particles within the tubes. This is due to high particle density and broad catalyst activity distribution (Zhang & Li, 2009, Bandaru et al., 2007). An interaction of the Fe particle and growing nanostructure at 930 ^oC favoring broad and straight nanotube formation is shown by the FE-SEM images. The CNTs XRD spectra (Figure 2a) showed crystallinity with the diffraction peak at 26.1^o ascribed to the graphite plane (002) reflection (Luo et al., 2015) with further small graphitic characteristic peaks at 43.7^o (100) and 44.7^o (101) (Song et al., 2016). The calculated $d_{(002)}$ interlayer spacing of ~0.33 nm is a typical value for CNTs (Kharissova & Kharisov, 2014), and it slightly decreases as expected with the increase in the CNTs' diameter (Algadri et al., 2017) as the CVD reaction temperature increased (Figure 1). The Raman spectra (Figure 2b) showed three distinct peaks D (~1341 cm^{-1}), G (~1571 cm^{-1}), and 2D (~2683 cm^{-1}) bands attributed to defects, graphitic mode, and overtone of D band, respectively (Rebelo et al., 2016). The $I_D\ I_G^{-1}$ ratios showed that multiwalled carbon nanotubes (MWCNTs) were formed (Andrade et al., 2015), defects decreased, and crystallinity increased as the reaction temperature increased (Rebelo et al., 2016). The G band and 2D band's defined intensity reflects the well-ordered stacking of layers of MWCNTs (Andrade et al., 2015).

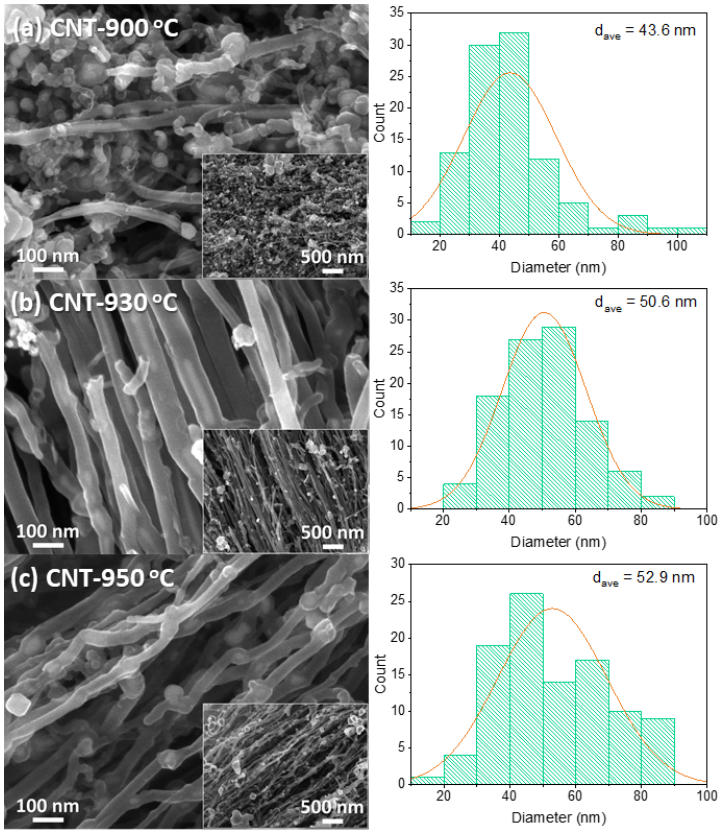

Figure 1: FE-SEM images and diameter distribution of carbon nanotubes synthesized at (a) 900 °C, (b) 930 °C, and 950 °C.

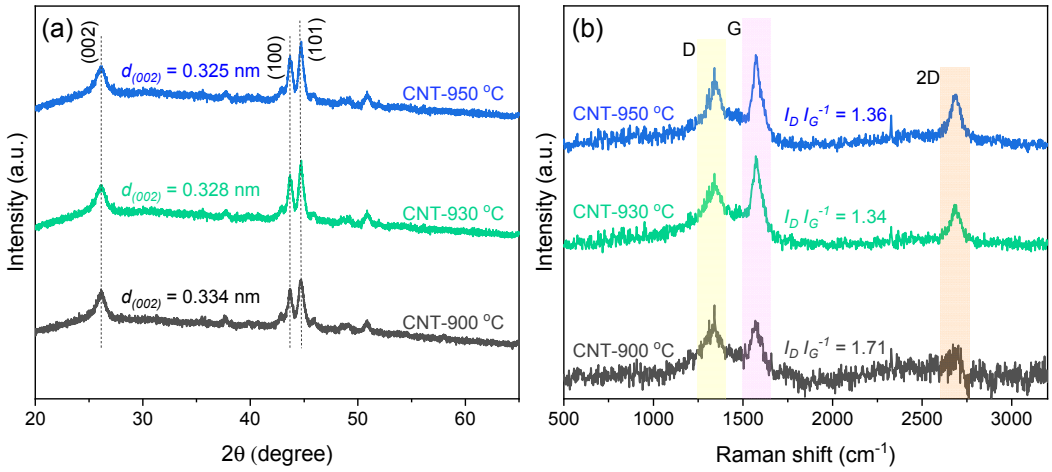

Figure 2: XRD (a) and Raman spectra (b) of carbon nanotubes synthesized at varied temperatures.

3.2 Nickel electroless plating of CNTs from PWO

The CNTs synthesized from CVD reaction temperature at 930 °C were purified prior to their further use for electroless plating (ELP). The purification method removed any amorphous carbon and particles as shown in the FESEM image (Figure 3a), and the decrease in $I_D\ I_G^{-1}$ ratio, the sharper and increased intensity of 2D peak (Figure 3b). The acid treatment also prepares the CNT surface for efficient ELP as it induced hydrophilic properties.

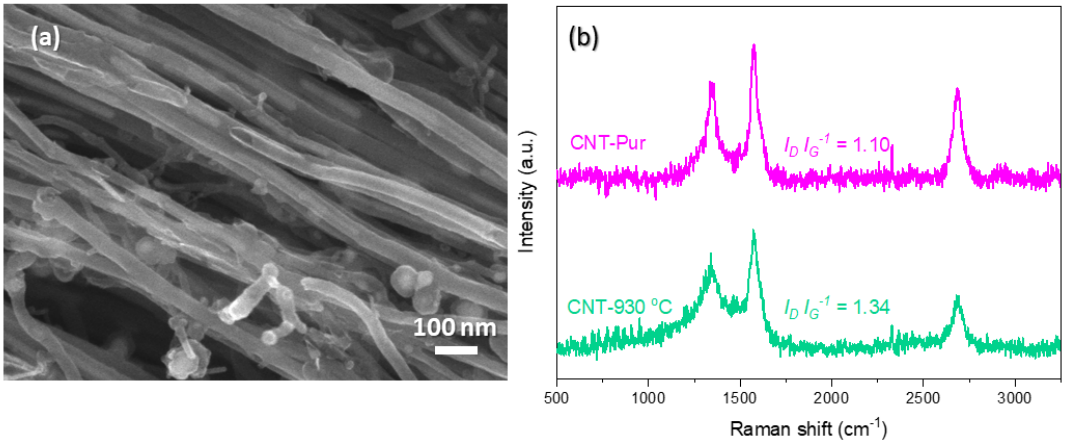

Figure 3: (a) FESEM image and (b) Raman spectra of the purified CNTs.

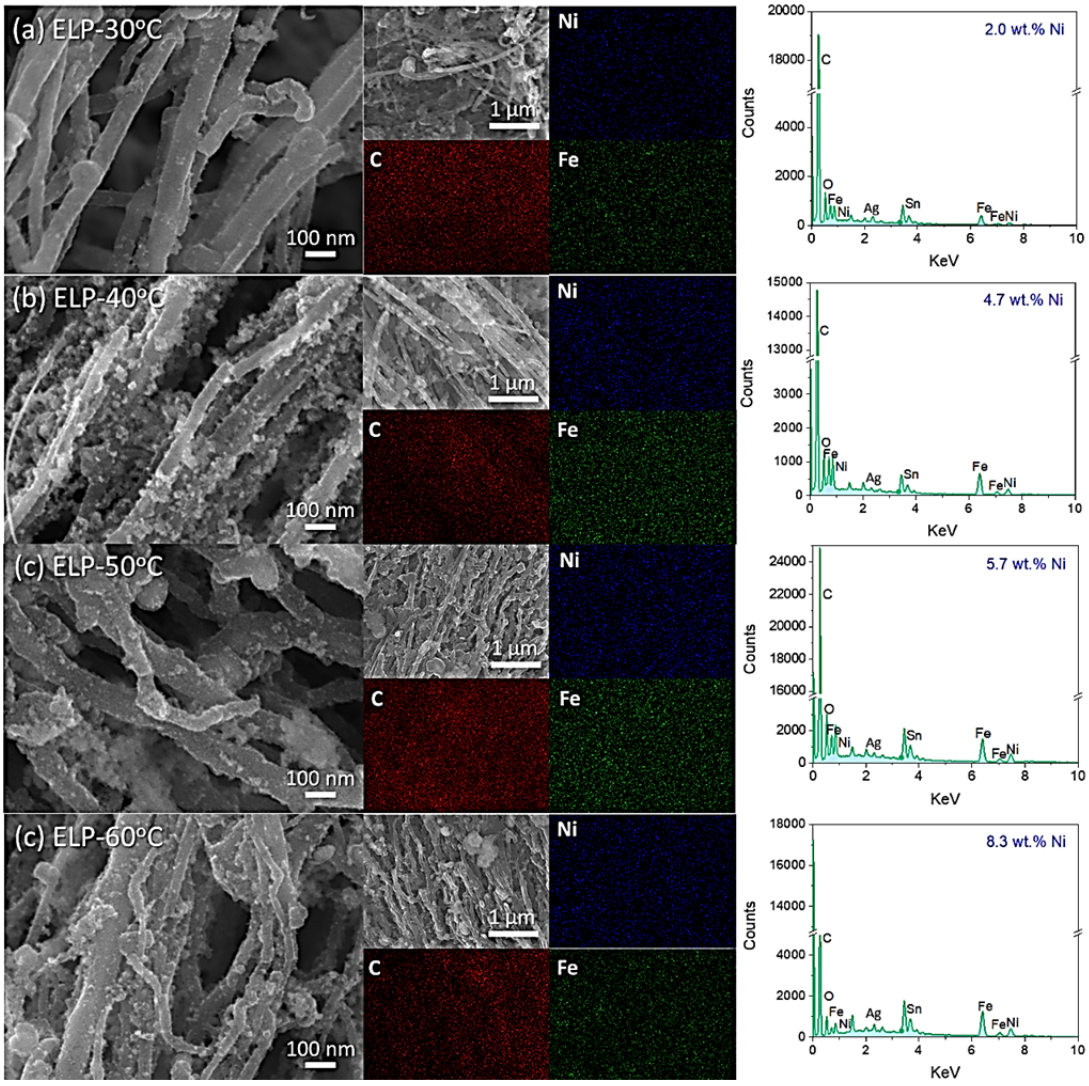

Figure 4: FE-SEM images, elemental (Ni, C, Fe) mapping, and EDX spectra of Ni-CNT composites prepared via electroless plating (ELP) at (a) 30 °C, (b) 40 °C, (c) 50 °C, and (d) 60 °C.

The ELP approach utilized a Palladium (Pd) free activation method and a relatively cheaper alternative in the form of $AgNO_3$. The Sn^{2+} adsorbed on the MWCNT surface during sensitization will reduce Ag^+ to Ag^0, enabling the CNT surface to be active for ELP (Equation 1, 16). The ELP can be surmised to follow two main reactions: (1) the spontaneous reduction of Ni via phosphite ions (Equation 2) (17) and non-spontaneous reduction of Ni (Equation 3) (Peng & Chen, 2012), hence the need of external energy. Ni deposition via ELP increased (2.0 – 8.3 wt. %) with increasing temperature (Figure 4). Fine Ni particles can be observed uniformly dispersed in the CNTs based on the FESEM images and elemental mapping (Figure 4).

$$Sn^{2+} + 2Ag^{+} \rightarrow Sn^{4+} + 2Ag^{0} \qquad E^0 = 0.65\ V \qquad (1)$$

$$Ni^{2}+H_2PO_2^-+H_2O \rightarrow Ni^0+H_2PO_3^-+H_2 \qquad E^0=0.26\ V \qquad (2)$$

$$Ni^{2+} + 2Ag \rightarrow Ni^0 + 2Ag^{+} \qquad E^0 = -1.04\ V \qquad (3)$$

During the deposition process, slower reaction rates can be surmised at a lower temperature (<30 °C) compared to a higher temperature (>30 °C). However, the deposition observed at 60 °C was very drastic, and the plating solution becomes turbid after a few minutes of deposition. This leads to the appearance of many fine Ni-globules (Figure 4c), which have a weak bond with the coating. It is suggested that these globules were generated by Ni particles' adsorption produced in the solution, rather than the Ni crystalline grain produced in-situ and grown on the CNT's surface. At lower temperatures, the slow and stable deposition rate resulted in uniform coatings (Figure 4a), which offer a robust physical sealing between the coating and the CNT. On the other hand, the Fe observed in the samples was from the catalytic vapor deposition of CNTs since Ferrocene was used as a catalyst.

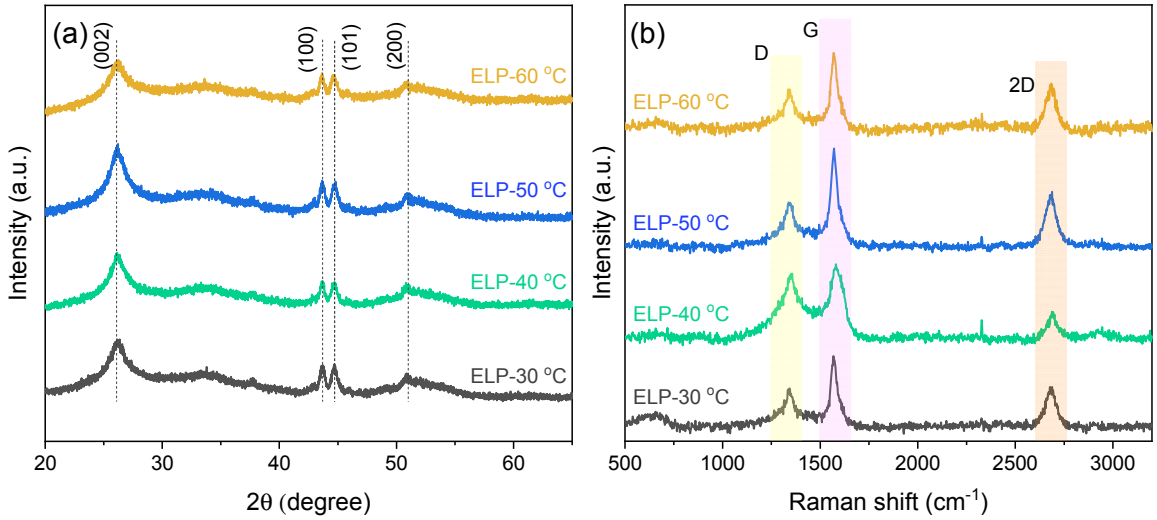

Figure 5: (a) XRD and (b) Raman spectra of Ni-CNT composites prepared via electroless plating (ELP) at varying temperatures.

The XRD pattern (Figure 5a) revealed the characteristic peaks for CNT (2θ = 26.18°) and the appearance of a broader peak at ~51° corresponding to Ni (Zhai et al., 2015, Xie et al., 2017). Peaks at 2θ = 43.2 °, 44.5°, and 51.8° are attributable to Ni(100), Ni(101), and Ni(200), respectively, and indicated the presence of the face-centered cubic phase of nickel (JCPDS 04-0850) and the crystalline nature of the layer. However, CNT's characteristic peak intensity slightly decreased after plating but did not significantly distort the crystalline phase. The ELP is a facile method of coating Ni onto CNTs surface. Its graphitic structure and order did not change substantially based on the relatively the same position and intensities of D, G, and 2D bands from the Raman spectra (Figure 5b). The slight increase of the G and 2D band as the plating temperature increased can be attributed to Ni's reinforcing effect on the crystallinity of CNT.

4. Conclusions

Upcycling of PWO was successfully done by producing CNT. A smooth and straight CNTs were successfully synthesized from PWO with ferrocene as a catalyst at a CVD reaction temperature of 930 °C. A relatively

cheaper and facile electroless coating of Ni via a Pd-free method was done at varying temperatures (30 – 60 ^{o}C). Ni deposition increased with increasing temperature due to enhanced metal ion reduction at a higher temperature without significantly distorting CNT's crystalline structure. The uniform coating of Ni to the as-synthesized CNT from PWO was achieved with potential use in catalytic applications.

Acknowledgments

This work is supported by Ratchadapisek Sompoch Endowment Fund (2015) of CU (CU-58-064-CC) and the National Nanotechnology Center (NANOTEC), NSTDA through the program of Research Network NANOTEC (RNN).

References

Algadri N. A., Hassan, Z., Ibrahim K., Bououdina M., 2017, Effect of ferrocene catalyst particle size on structural and morphological characteristics of carbon nanotubes grown by microwave oven. Journal of Materials Science, 52(21), 12772–12782.

Andrade N. F., Vasconcelos T. L., Gouvea C. P., Archanjo B. S., Achete C. A., Kim, Y. A., Endo, M., Fantini, C., Dresselhaus, M.S., Souza Filho, A. G., 2015, Linear carbon chains encapsulated in multiwall carbon nanotubes: Resonance Raman spectroscopy and transmission electron microscopy studies. Carbon, 90, 172–180.

Bandaru P. R., Daraio C., Yang K., Rao A. M., 2007, A plausible mechanism for the evolution of helical forms in nanostructure growth. Journal of Applied Physics, 101(9), 094307.

Dang L., Hou, Y., Song C., Lu Q., Wang Z., Feng Q., Lu Q., Gao F., (2018). Space-confined growth of novel self-supporting carbon-based nanotube array composites. Composites Part B: Engineering.

Hernández-Vargas J., Martinez-Gomez J., González-Campos J., Lara-Romero J., Ponce-Ortega J., 2015, Optimal Processing of Carbon Nanotubes, Chemical Engineering Transactions, 45, 1183-1188.

Kharissova O. V., Kharisov B. I., 2014, Variations of interlayer spacing in carbon nanotubes. RSC Adv., 4(58), 30807–30815.

Ko S., Lee C. W., Im J. S., 2016, Petrochemical-waste-derived high-performance anode material for Li-ion batteries. Journal of Industrial and Engineering Chemistry, 36, 125–131.

Lam S. S., Liew R. K., Jusoh A., Chong C. T., Ani F. N., Chase H. A., 2016, Progress in waste oil to sustainable energy, with emphasis on pyrolysis techniques. Renewable and Sustainable Energy Reviews, 53, 741–753.

Liu X., Yao T., Lai R., Xiu J., Huang L., Sun S., Luo Y., Song Z., Zhang Z., 2019, Recovery of crude oil from oily sludge in an oilfield by sophorolipid, Petroleum Science and Technology, 37:13, 1582-1588.

Luo X.-F., Yang C.-H., Peng Y.-Y., Pu N.-W., Ger M.-D., Hsieh C.-T., Chang J.-K., 2015, Graphene nanosheets, carbon nanotubes, graphite, and activated carbon as anode materials for sodium-ion batteries. Journal of Materials Chemistry A, 3(19), 10320–10326.

Mukherjee P. K., 2019, Influence of carbon nanotubes in antiferroelectric liquid crystals. Soft Materials, 1–7.

Peng Y., Chen Q., 2011, Fabrication of Copper/Multi-Walled Carbon Nanotube Hybrid Nanowires Using Electroless Copper Deposition Activated with Silver Nitrate. Journal of The Electrochemical Society, 159(2), D72–D76.

Rebelo S. L. H., Guedes A., Szefczyk M. E., Pereira A. M., Araújo J. P., Freire C., 2016, Progress in the Raman spectra analysis of covalently functionalized multiwalled carbon nanotubes: unraveling disorder in graphitic materials. Physical Chemistry Chemical Physics, 18(18), 12784–12796.

Singh P., Jain R., Srivastava N., Borthakur A., Pal D. B., Singh R., Madhav S., Srivastava P., Tiwary D., Mishra P. K., 2017, Current and emerging trends in bioremediation of petrochemical waste: A review. Critical Reviews in Environmental Science and Technology, 47(3), 155–201.

Song J., Zhu C., Fu S., Song Y., Du D., Lin Y., 2016, Optimization of cobalt/nitrogen embedded carbon nanotubes as an efficient bifunctional oxygen electrode for rechargeable zinc–air batteries. Journal of Materials Chemistry A, 4(13), 4864–4870.

Xie Y., Lu L., Tang Y., Zhang F., Shen C., Zang X., Ding X., Cai W., Lin L., 2017, Hierarchically nanostructured carbon fiber-nickel-carbon nanotubes for high-performance supercapacitor electrodes. Materials Letters, 186, 70–73.

Zhai T., Liu B., Ding C.-H., Lu L.-X., Zhang C., Xue K.-G., Yang D.-A., 2015, Ni–P electroless deposition directly induced by sodium borohydride at interconnected pores of poly (ether ether ketone)/multiwalled carbon nanotubes composites surface. Surface and Coatings Technology, 272, 141–148.

Zhang M., Li J., 2009, Carbon nanotube in different shapes. Materials Today, 12(6), 12–18.